

Article

Descriptive Process Mineralogy to Evaluate Physical Enrichment Potential of Malatya/Kuluncak Rare Earth Ore through MLA

Burakhan Ersoy¹, Mehmet Umut Beşirli¹, Selim Topal², Belma Soydaş Sözer³ and Fırat Burat^{1,*}

¹ Department of Mineral Processing Engineering, Faculty of Mines, Istanbul Technical University, Istanbul 34469, Türkiye; ersoyb18@itu.edu.tr (B.E.); besirli17@itu.edu.tr (M.U.B.)

² Department of Academic and Publications, Turkish Energy, Nuclear and Mineral Research Agency (TENMAK), Ankara 06980, Türkiye; selim.topal@tenmak.gov.tr

³ Rare Earth Elements Research Institute, Turkish Energy, Nuclear and Mineral Research Agency (TENMAK), Ankara 06980, Türkiye; belma.soydassozer@tenmak.gov.tr

* Correspondence: buratf@itu.edu.tr; Tel.: +90-21-2285-7359

Abstract: Rare earth elements (REE) are indispensable for industries such as magnetic, phosphorus, metal alloys, catalysts, ceramics, glass, polishing and defense systems due to their unique physical and chemical properties. Currently, China is the largest supplier in the world, accounting for production of more than 95% of the world's rare earth oxides (REO). To reduce the influence of China on the REE market, some countries have started to develop their own national strategies for the production and use of REE-bearing resources. Within the scope of this study, particle size, chemical, MLA, XRD, and SEM-EDS analysis were performed for material characterization, and shaking table, centrifugal, and magnetic separations were carried out for the beneficiation of Malatya/Kuluncak rare earth ore. The XRD analysis indicated that the representative sample consisted of major minerals such as albite, calcite, montmorillonite, muscovite, titanite, kaolinite, clinocllore, and aegirine. Parisite, bastnaesite, Zr-REE-Silicate, Fe-REE-Oxide, and Ca-Ti-Nb-REE-Oxide were detected as REE-bearing minerals by MLA. The chemical analysis resulted in a Σ REO grade of 3628 g/t, and the ore consisted mostly of light REEs. According to the results of the gravity separation for the coarsest fraction, about 11.3% by weight of the total feed was concentrated as a heavy product with 6437 g/t Σ REO content. As a result of magnetic separation, magnetic products with 5561 g/t and 6013 g/t Σ REO were obtained as coarse and fine fractions, respectively. Finally, the characterization studies and enrichment results were correlated, and very important and meaningful indications about the behavior of REE-bearing minerals were obtained.

Keywords: rare earth elements; characterization; physical separation; MLA



Citation: Ersoy, B.; Beşirli, M.U.; Topal, S.; Sözer, B.S.; Burat, F. Descriptive Process Mineralogy to Evaluate Physical Enrichment Potential of Malatya/Kuluncak Rare Earth Ore through MLA. *Minerals* **2023**, *13*, 1197. <https://doi.org/10.3390/min13091197>

Academic Editor: Kevin Galvin

Received: 18 July 2023

Revised: 6 September 2023

Accepted: 11 September 2023

Published: 12 September 2023



Copyright: © 2023 by the authors. Licensee MDPI, Basel, Switzerland. This article is an open access article distributed under the terms and conditions of the Creative Commons Attribution (CC BY) license (<https://creativecommons.org/licenses/by/4.0/>).

1. Introduction

In parallel with technological development, critical elements are used on a large scale in high-technology sectors. This situation requires the selective processing of minerals containing rare earth elements (REEs) in much higher amounts. The lanthanide group of elements in the periodic table is named REE, and the atomic numbers of these 15 elements range from 57 (La) to 71 (Lu). Sc and Y are included in this group due to chemical properties similar to those of the lanthanides, which are divided into two sub-groups, called light REE (LREE) and heavy REE (HREE) [1]. In nature, there are more than 250 rare earth minerals (REMs) in the form of carbonatites, oxides, phosphates, silicates, and halides. Bastnaesite ((Ce, La)CO₃F) and Monazite ((Ce, La, Nd, Th)PO₄) are the main REE-bearing ores, and about 95% of the world's rare earth resources are associated with these minerals [2].

Supply security, discovery and development of new deposits, substitute materials, recycling, economic policies, technical knowledge and experience (R&D and mining practice),

waste management culture, and individual global power and influence are important factors that shape the REE strategies of many countries [3]. In recent years, REEs have become extremely important worldwide due to their unique magnetic, phosphor, and catalytic properties. They contribute to many technical aspects such as lower energy consumption, higher efficiency, durability, and thermal stability. Computers, mobile phones, televisions, energy-saving lamps, and wind turbines all contain REEs in certain amounts. They are an indispensable resource for high-tech equipment such as lasers, superconducting magnets, and hybrid car batteries. For this reason, the enrichment possibilities of rare earth deposits discovered in recent years with various processing technologies have attracted a great deal of scientific and industrial interest. The use of REEs in magnets and catalysts accounts for almost 50% of total demand, and China dominated the market with 84% of production in 2016. Similarly, China continues this dominance according to the USGS (2023), and accounts for 70% of global production and 34% of global reserves [4]. Therefore, the exploration and development of new REE deposits have gained importance to providing supply security and diversification of the deposits globally. Especially after the export restrictions by China in 2010, the evaluation of alternative and domestic REE resources gained importance across the world. Türkiye is one of the countries starting exploration and beneficiation studies for REE production. With the research and studies of the sole nationwide REE Institute (TENMAK, NATEN), the General Directorate of Mineral Research and Exploration (MTA) and the General Directorate of ETİMADEN are contributing to these studies to unearth these valuable and strategically important elements. The Eskişehir/Beylikova REE deposit has been studied in terms of beneficiation possibilities, and a pilot-scale plant construction project was started to process this important REE deposit. Many new deposits that are being explored are poorly processed but contain very valuable minerals. One of these deposits is Kuluncak, and it is Türkiye's second largest REE source after Beylikova.

REE ores can occur in carbonatite, alkaline complexes and pegmatites, felsic volcanic deposits, granites and granitic pegmatites, iron oxide copper gold (IOCG) deposits, granite-related skarns, carbonatite-related skarns, hydrothermal deposits, heavy mineral sands, laterite/soil/clays, shale hosted deposits, alluvial/placer deposits, sedimentary deposits and tailings [5]. The only three main REE-bearing minerals currently in commercial use are bastnaesite, monazite, and xenotime. Of these three minerals, monazite and xenotime are found in heavy mineral sand deposits where they require little or no comminution, and their economic beneficiation processes are well-developed. Bastnaesite is economically extracted on a large scale in Mountain Pass, USA and Bayan Obo, China.

The Hekimhan-Hasançelebi-Kuluncak region in Türkiye is located within the Anatolide-Tauride Belt and contains Cretaceous-Paleocene alkaline magmatic and volcanic rocks [6]. Özgenç et al. [7] classified Başören carbonatites as early-phase aegirine-fluorite-apatite carbonatites (C1) and late-phase fluorite-apatite carbonatites (C2); C1 and C2 are economic fluorite-bearing and britholite-bearing type carbonatites, respectively. They stated that economic britholite occurrences are in nepheline syenites and contain 57% REEs, while LREEs generally occur in carbonatites. As reported by Akiska et al. [8] carbonatite is the last stage of intrusion in Başören, which caused the fenitization of syenites and the occurrence of britholite and fluorite in low quantities. According to their study, the main Th- and REE-bearing minerals were identified as bastnaesite, britholite, and thorite containing high amounts of Th and REEs.

Within the project area, Early Cretaceous–Late Paleocene aged Kuluncak-Hasançelebi feldspathic lava is dominant within the area encircling Kuluncak, Darılı, and Başören villages. Nephelinitic lava is represented by nephelinite syenite, sodalite syenite, alkyl syenite, syenite, micro syenite, and nephelinite syenite pegmatite with coarse albite and aegirine type of rocks. Syenitic rocks cover an area of 4 km² and have equal size, medium grain, and holocrystalline texture. The rock consists of alkaline feldspar, plagioclase, pyroxene crystals, and pseudomorphs with holocrystalline texture [9]. Feldspathic rocks and carbonatitic lava related to these rocks are REE-bearing rocks, in which REEs occurred across contact pneumatolytic activity and skarn zones following contact metamorphism,

contact metasomatic alteration zones, and fenitization zones in the pegmatitic period and are also associated with fluorite through hydrothermal activity.

Many minerals contain REEs; however, they are typically found in small-scale deposits where data are difficult to obtain and the task of determining general separation characteristics is even more difficult. The enrichment of REE-bearing minerals is a topic that requires much more research to fill the knowledge gaps in emerging rare earth studies. Regarding the recovery of REEs from primary sources, many variables need to be investigated depending on the ore, method, and equipment. Physical and physicochemical enrichment processes of REEs can be performed using gravity, magnetic, electrostatic separation, and flotation methods [10]. The most important ore-related factors affecting the success of the beneficiation processes are the REE mineral type, particle liberation size, and the structure of the gangue minerals. Although REE-bearing minerals occur in the same deposit, their properties may differ. In other words, each deposit can be approached with a different process and method.

In hydrometallurgical processes, the presence of impurities such as iron increases inorganic acid consumption and associated operating costs. In addition, there are environmental disadvantages and energy costs caused by the use of high temperatures in pyrometallurgical processes. Physical enrichment methods have a very important place in the ore processing industry due to their various advantages, such as low cost, easy operation, and lower environmental impact compared to physicochemical and chemical methods. For this reason, physical methods are generally applied before chemical processes to produce a pre-concentrate with a high recovery rate and a rejectable waste with a low metallic quality. Gravity separation has been widely used for a long time in the mineral processing industry for the separation of valuable minerals from the host rock. Low capital and operating costs draw increased attention to these methods [11,12]. REE enrichment from heavy mineral sands is common in gravity separation processes, where spirals and shaking tables are widely used. This is quite successful with conventional gravity equipment due to the relatively high specific gravity of REEs (up to 7 g/cm³) and the low specific gravity of silicate gangue (2.5 g/cm³) [13]. Apart from heavy mineral sand beneficiation, gravity separation methods (shaking tables, spiral concentrators, and conical separators) have been used to separate bastnaesite and monazite from the iron-bearing and silicate gangue material before flotation in the world's largest REE mine (Bayan Obo, China) [14,15]. However, one of the difficulties with the gravitational separation of Bayan Obo ore is that gangue minerals (e.g., barite) escape into the heavy product because they have a specific gravity similar to that of the REE-bearing minerals.

Processing fine particles by conventional gravity methods is challenging because the buoyancy of water reduces the gravity difference between the particles to be separated, reducing selectivity in separation. Despite their high specific gravity, particles that are liberated in very fine sizes (especially below 75 µm) cannot be concentrated in heavy products using conventional gravity separators such as shaking tables and spirals, and very fine heavy-metal particles are lost with the light fraction. Centrifugal gravity separators such as the multi gravity separator (MGS) [16], Knelson [17], and Falcon [18] operating at high rotational speeds and exerting enormous G forces (G-force) on the particles can be used effectively to eliminate this negative situation caused by very fine liberated particles in classical gravity separation systems and to capture the minerals with high specific gravity escaping into the light fraction.

Since many REEs are strongly paramagnetic, magnetic separation is a highly effective technique for REM enrichment. Gd, Tb, Dy, and Tm show ferromagnetic properties, while Sc, Y, La, and Lu are diamagnetic REEs, and the others paramagnetic [19]. Magnetic separation is commonly applied to separate diamagnetic minerals such as fluorite and quartz from ferromagnetic (such as siderite) and paramagnetic minerals (such as monazite, bastnaesite, and xenotime) [20,21]. A low magnetic density can be used to capture ferromagnetic particles, while a high magnetic density must be preferred for paramagnetic minerals with lower magnetic susceptibility. There are many studies in the literature on gravity separa-

tion combined with magnetic separation [22,23]. Magnetic separators are very effective in monazite enrichment from beach sands. In the first stage, strong magnetic minerals such as magnetite are removed, and then monazite is separated from non-magnetic heavy mineral gangue material, zircon, and rutile. Jordens et al. [22] performed a pre-concentration process including Knelson and Falcon centrifugal concentrators followed by high-intensity wet drum magnetic separation steps as well as dry-induced roll magnetic separation and wet high-intensity magnetic separation steps. Characterization tests and analysis identified several silicates including biotite, plagioclase, quartz, K-feldspar, Fe-oxides (both magnetite and hematite), lesser proportions of muscovite/clays, chlorite, amphibole, carbonates, and trace proportions of other minerals (e.g., fluorite). They reported that REM recovery from this ore using centrifugal equipment was effective, but the recovery decreased as the particle size decreased. Thompson et al. [24] reported that neither the shaking table nor the Falcon concentrator provided a preferential upgrading of REE-bearing minerals, even at $-38\ \mu\text{m}$ [24]. Mineralogical analysis showed that composite particles containing higher proportions of dolomite and quartz resulted in higher REE losses. Lab-scale gravity separations have been successfully performed on Türkiye's largest deposit with finely grained mineralization. The pre-concentration of Beylikova ore with an average REO content of 3.42% was provided by attrition and scrubbing. Rough concentrate was upgraded using MGS, and as a result, a bastnaesite concentrate with 35.5% REO grade and 48% recovery was produced [16]. One of the most important findings of this study is that the liberation size of REEs is below $5\ \mu\text{m}$. The use of Knelson or Falcon concentrators, which can apply more G force on the grain, may provide a solution for the enrichment of finely dispersed REE ores. Hedrick et al. [25] produced a pre-concentrate by performing a series of physical enrichment processes (gravity and electromagnetic separation) for the recovery of loparite (Ce, Na, Sr, Ca)(Ti, Nb, Ta, Fe⁺³)O from igneous feldspathic ore located in Lovozero Alkali Massif, Russia [25]. Loparite is hosted with aegirine, apatite, eudialyte, feldspar, nepheline, ramsayite, and titanite. The primary ores contain 2 to 3% loparite, and the REO content of the loparite ranges between 30 and 36%. The ore is concentrated to 95% loparite through a combination of gravitational and electromagnetic separation techniques. As by-products, an average of 97% pure aegirine concentrate and a nepheline-syenite concentrate containing 20.7% nepheline and 31.7% feldspar were produced. Thus, an economic contribution is provided not only from REEs but also from other by-products.

Today, flotation is the most important pre-enrichment method used to concentrate bastnaesite, monazite, xenotime, parisite, and other REMs by using different hydroxamic acids and fatty acids as collectors. However, these reagents can also float some gangue minerals such as iron oxide minerals [26]. Physical separation methods such as gravity and magnetic separation are preferred to remove these gangue minerals before or after flotation. Due to the high investment, the complexity of the process, and the use of a large number of reagents, flotation mainly follows physical beneficiation; thus, a high REE-containing concentrate can be obtained in this way. Yang et al. [2] studied the enrichment of a complex rare earth element (REE) ore containing carbonates, silicates, oxides, and other REEs (e.g., zircon and pyrochlore) by flotation and high gradient magnetic separation (HGMS) [2]. SEM images of REE-bearing minerals showed fine grains of bastnaesite, synchisite, parisite, britolite, pyrochlore, and zircon. Compared to flotation, HGMS was significantly less selective for the recovery of La and Ce. Therefore, more than one separation process must be preferred for the enrichment of this type of ore with a complex structure.

The beneficiation of REE minerals can involve many different beneficiation unit operations, but the final process selection typically depends on the natural mineral properties [27]. Xu et al. [28] used the mineral liberation analysis (MLA) technique to provide and evaluate the liberation characteristics of the Weishan REE ore. According to the mineralogical study results, the major REE minerals were bastnaesite, monazite, xenotime, and a small amount of parisite. The degree of release of bastnaesite and monazite was 79.65% and 75.67%, respectively, below the $75\ \mu\text{m}$ fraction. In another study, Baştürkçü et al. [29] utilized MLA to reveal the effects of mechanical attrition on Eskişehir-Beylikova REE ore. Mechanical

attrition has notable effects from the point of enhancement of liberated particles and the decrement of binary and ternary associations. More than 10% free surface was achieved in this way. A detailed report on the process mineralogy and physical enrichment process of Malatya/Kuluncak rare earth minerals has not yet been presented or published. According to a limited number of studies in the literature, REEs in Malatya-Kuluncak ore are accumulated in very fine size fractions. Process parameters such as mineral composition, element formation status, mineral particle size distribution, mineral association, and liberation size were analyzed by MLA to provide detailed primary theoretical data for further improvement of the physical beneficiation process for Malatya/Kuluncak rare earth ore.

2. Material and Methods

2.1. Material

A drill core sample of around 200 kg supplied from the Kuluncak region of Malatya province was transferred to Istanbul Technical University, Mineral Processing Engineering Department Pilot Plant Laboratory. Before the characterization and enrichment studies, a multi-stage crushing process was applied using jaw, cone, and roller crushers to provide sufficient liberation of particles. The representative ore samples and the location map of the projected field are presented in Figure 1.



Figure 1. A representative sample (a) and the location of the deposit (b).

2.2. Methods

Ore characterization was carried out through particle size distribution (PSD), X-ray diffraction (XRD), mineral liberation analysis (MLA), ICP-MS (mass spectrometry), and X-ray fluorescence (XRF) analysis. After the gradual size reduction process was completed, representative ore samples were prepared by the quartering method. Wet sieve analyses were carried out to determine the size distribution characteristics of the comminuted ore samples. The REE contents of the representative ore sample and products were determined using inductively coupled plasma mass spectrometry (ICP-MS) (Agilent 7800 model) following lithium metaborate/tetraborate fusion and solubilization in nitric acid. The main oxide components were analyzed using the XRF equipment (Panalytical Axios max). The XRD (Bruker D8 Advance Powder X-ray Diffractometer) analysis was carried out at the geology department of Istanbul Technical University for the identification of the crystal structure of the material.

MLA studies were completed on the run-of-mine ore sample to determine the mineral boundaries with a combination of scanning electron microscope (SEM), energy dispersive X-ray spectra (EDS), and advanced MLA software for obtaining, processing, and analyzing images in terms of particle sizes and mineral identification. MLA was performed using FEI MLA 650 and FEI Quanta 400 MLA instruments with a Bruker X-Flash dual EDS system. The analyses were conducted in the MTA (General Directorate of Mineral Exploration and Research) Mineralogy-Petrography Research Laboratory. The representative sample ground below 150 μm and cold molding rosin (4 units of rosin + 1 unit of hardener) were poured into 30 mm molds, mixed, and left to turn into solid. Entirely solidified samples were removed from the molds, and their surfaces were polished in approximately eight stages through an automatic abrading-polishing machine. Following this process, the surfaces of the polished samples were covered up with carbon before being placed in the MLA device. Following control and calibrations, the device was run for analysis. Backscatter electron (BSE) images were taken automatically for all particles (minerals) in all fractions at this stage, and chemical analysis (EDS) data of points consisting of different compositions on each particle were collected. After the data were collected automatically, mineral definition, mineral classification, and separation of artificially locked particles were carried out, respectively. Finally, mineral reference, modal mineralogy, calculated assay, elemental distribution, mineral liberation, and other data were derived, produced, and reported.

2.3. Beneficiation Methods

In the experimental studies, separation processes were carried out according to specific gravity and magnetic susceptibility differences to obtain an REE concentrate. The methods applied in this study were not final, since the main purpose of this study was to characterize this ore in detail, which has not previously been studied in the literature for beneficiation purposes, and to examine the possibility of producing a high-metal-content pre-concentrate before hydro/pyrometallurgical processes. A material composed of two or more components having a marked specific gravity difference between them is generally enriched in sizes ranging between 3 and 0.1 mm using a shaking table. In this context, the crushed material below 1 mm was classified as $-1 + 0.3$ mm, $-0.3 + 0.074$ mm, and -0.074 mm and subjected to the gravity separation experiments. While the $-1 + 0.3$ mm and $-0.3 + 0.074$ mm size fractions were fed into the shaking table, the fine fraction, -0.074 mm, was fed to the centrifugal separators. The laboratory-type Wilfley shaking table used in the enrichment studies is manufactured of a fiberglass deck with a rectangular shape (800 mm in length and 400 mm in width). The inclination of the table can be adjusted easily. Thus, with this differential movement, the particles in contact with the surface of the table are moved by friction from the feeding zone on the right to the left. The riffles, which are 6 mm high on the right side of the deck (the feed section), decrease toward the left side (the concentrate section). Two water sources are placed on the deck as feed and wash water. With the water current moving from top to bottom, the light and coarse grains are caught by the drag force of the water and leave the table faster by crossing the riffles. Heavy and fine grains, on the other hand, are taken from the farthest point on the left of the table by not passing over the riffles. The test conditions were as follows: 10 L/min wash water, 2 mm stroke length, 300 cycles per min frequency, 3° lateral angle for coarse and 2° for fine fraction, 30 kg/h feed rate. At the end of the experiments, three products, namely concentrate (heavy), middling, and tailing (light), were obtained using two splitters.

Two different types of centrifugal separators, MGS and Knelson concentrator, which have different operating parameters and structures, were chosen to concentrate REEs. MGS tests were performed with a Mozley C900 model lab/pilot-scale concentrator. It rotates at different speeds (90–250 rpm) and enables the generation of 5–15 G-force on the particle surface. A scraper assembly is mounted inside of the drum, driven in the same direction, and slightly faster than the drum. Solids with high specific gravity (concentrate) accumulating on the inner wall of the drum are scraped off toward the opposite direction

of flow. Materials with lower specific gravity (tailings) move toward the rear of the drum. Secondly, a laboratory-type Knelson concentrator (KC-MD3 model) that can reach up to 80 times G-force was used. The lighter particles overflow from the upper part of the bowl, and heavy fractions stick to the bowl liner. The bowl liner of this equipment has some rings to trap the heavy particles. The fluidization water can be adjusted between 0 and 8 psi. Thus, heavy and light products with different amounts and contents can be obtained.

Magnetic separation experiments were employed using a laboratory-type dry high-gradient rare earth magnetic separator (REMs) with a magnetic field of 4000 Gauss (G). For the coarse fraction, $-1 + 0.3$ mm, the band speed and splitter angles were chosen at 100 rpm and 95° – 110° , respectively. The optimum parameters were determined as 110 rpm band speed and 90° – 110° splitter angles for the $-0.3 + 0.074$ mm size fraction. The recovery rate used to evaluate and discuss the experimental results was calculated with the following Equation (1).

$$R (\%) = (C_c/F_f) 100 \quad (1)$$

where C is the weight of the concentrate, c is the metal content of the concentrate, F is the weight of the feed, and f is the metal content of the feed.

3. Results and Discussion

In this section, the distribution and content of REEs, mineral associations, and liberations are explained by characterization methods and correlated with the behavior of REE-bearing minerals in the physical enrichment processes.

3.1. Characterization Studies

The comminuted samples were subjected to wet sieve analyses, and three PSD curves were generated. The d_{80} values of the crushed samples after the jaw, cone, and roll crusher were determined as 8.1, 3.3, and 0.54 mm, respectively. The analysis results for the REEs are given in Table 1. In total, the representative ore sample contained about 3628 g/t REOs and approximately 237 g/t ThO₂, and 272 g/t U₃O₈ as the radioactive components. The ratio of heavy HREOs to LREOs was about 24%. According to the XRF results, the ore was composed of the oxides SiO₂, Al₂O₃, Fe₂O₃, CaO, Na₂O, K₂O, ZrO₂, TiO₂, and MgO in fractions of 53.05%, 13.95%, 7.68%, 6.49%, 6.11%, 2.38%, 0.82%, 0.68%, and 0.40%, respectively.

Table 1. LREO and HREO contents of the Kuluncak ore sample.

LREOs		HREOs	
Oxide	Content, g/t	Oxide	Content, g/t
Sc ₂ O ₃	35	Y ₂ O ₃	518
La ₂ O ₃	951	Gd ₂ O ₃	43
Ce ₂ O ₃	1464	Tb ₂ O ₃	8
Pr ₂ O ₃	130	Dy ₂ O ₃	58
Nd ₂ O ₃	298	Ho ₂ O ₃	14
Sm ₂ O ₃	45	Er ₂ O ₃	49
Eu ₂ O ₃	9	Tm ₂ O ₃	7
		Yb ₂ O ₃	38
		Lu ₂ O ₃	4
Total	2932	Total	696

The results of the XRD analysis are presented in Figure 2. The sample consisted of major minerals such as Albite (NaAlSi₃O₈), Calcite (CaCO₃), Montmorillonite (Ca_{0.2}(Al, Mg)₂Si₄O₁₀(OH)₂·4H₂O), Muscovite ((K, Na)(Al, Mg, Fe)₂(Si₃·Al_{0.9})O₁₀(OH)₂), Titanite (CaTiO(SiO₄)), Kaolinite (Al₂Si₂O₅(OH)₄), Clinocllore ((Mg₅Al)(Si,Al)₄O₁₀(OH)₈), and Aegirine (NaFeSi₂O₆). The ore composition mostly consisted of aluminosilicates, and the ore had a clayey structure. The ferrous content mainly originated from the aegirine mineral.

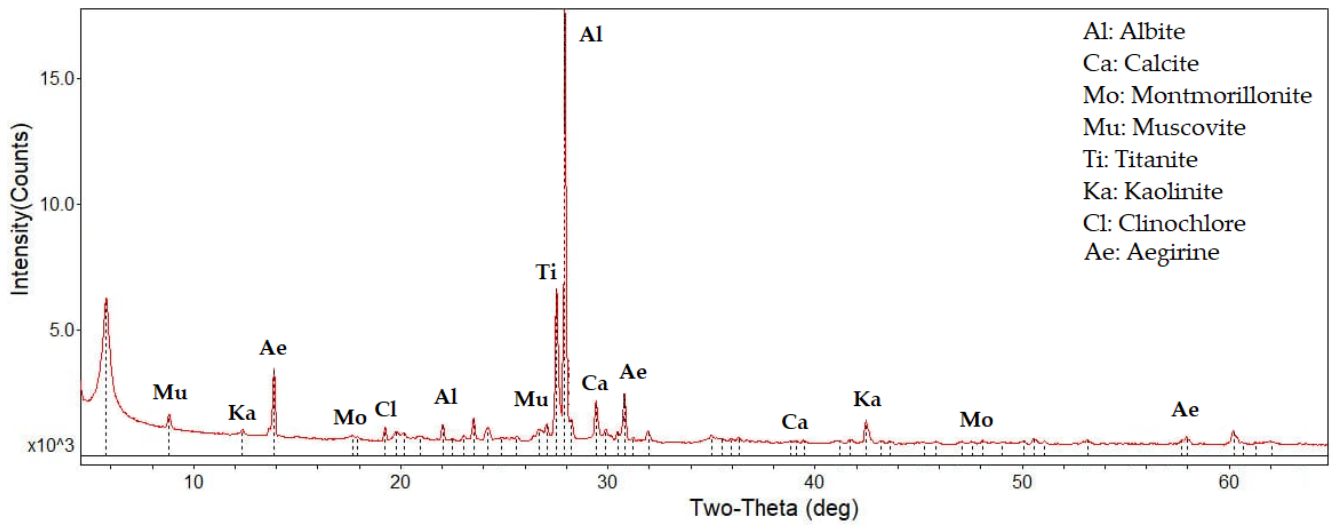


Figure 2. The XRD spectrum of the representative sample.

For further identification, MLA was performed on the various fractions. An average of 30,000 particles were counted for each fraction. Thus, the REE minerals were defined, and mineral associations, modal mineralogy, and mineral liberation by the free surface of raw samples were identified. Regarding modal mineralogical composition defined through MLA (see Figure 3), the dominant gangue minerals in the ore composition were determined as aluminosilicates (albite and K-feldspar) and iron-silicates (aegirine). The high silicate composition observed through MLA tests confirmed the XRD results and chemical analysis tests. Since REE-bearing minerals were low in quantity, they were classified under the title of “other minerals”.

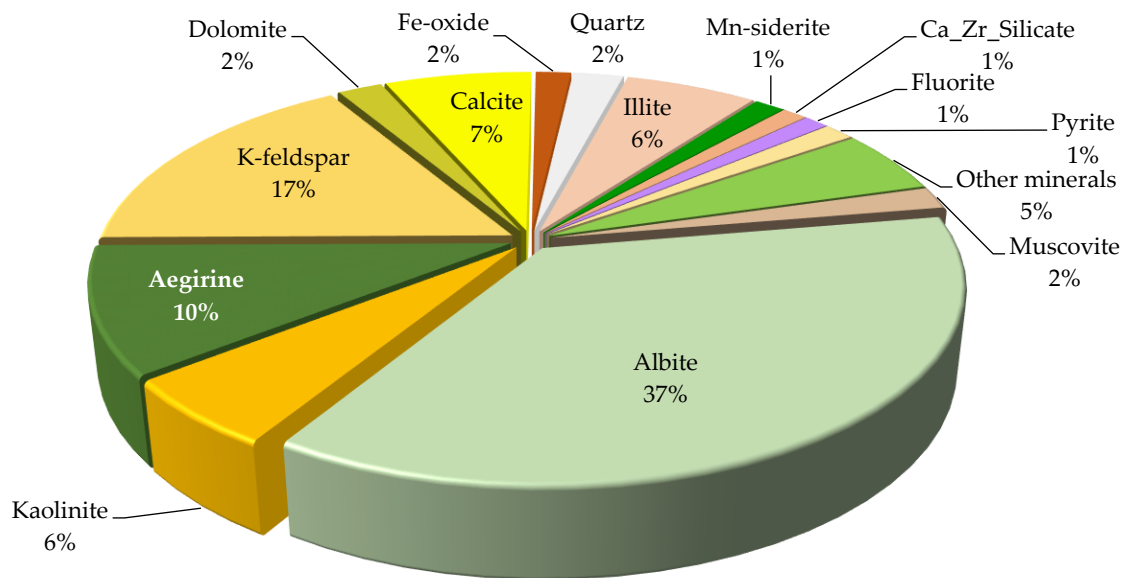
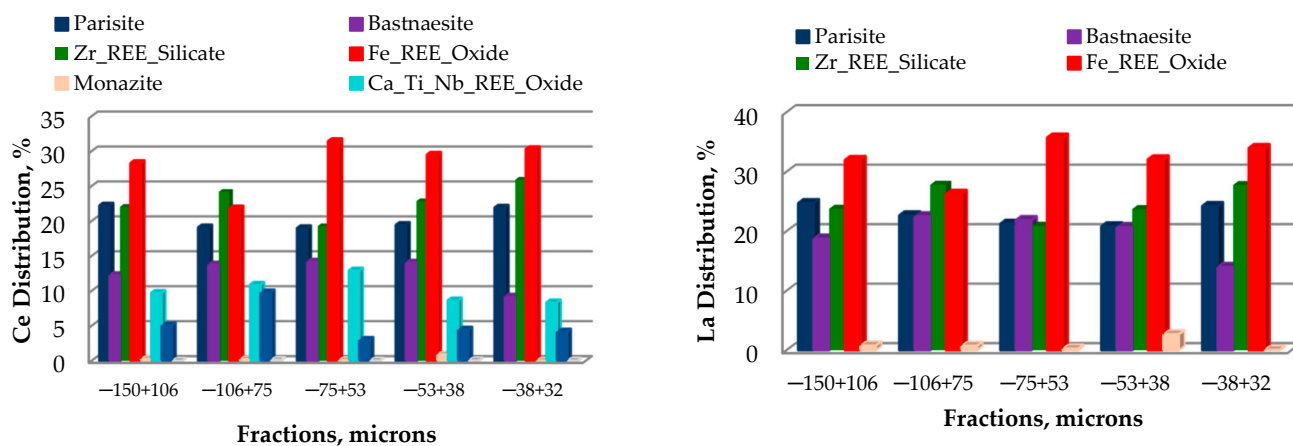


Figure 3. Modal mineralogy of the raw sample.

Parasite, bastnaesite, Zr-REE-Silicate, Fe-REE-Oxide, and Ca-Ti-Nb-REE-Oxide were detected as the main REE-bearing minerals in the ore composition. As shown in Table 2, REE-bearing mineral content was around 1% (~11,000 g/t) in total. Elemental distribution results in Figure 4 indicate that Fe-REE-Oxide, Zr-REE-Silicate, parasite, and bastnaesite were the dominant minerals for Ce. Similarly to Ce, Fe-REE-Oxide was the dominant mineral for La. MLA results also revealed elements such as Zr, Th, and U that may have significant economic potential.

Table 2. REE-bearing mineral contents by the size fraction.

Mineral	Size Fractions, μm					Weighted Average, g/t
	−150 + 106	−106 + 75	−75 + 53	−53 + 38	−38 + 32	
Parisite	0.17	0.15	0.13	0.15	0.16	1522
Bastnaesite	0.13	0.15	0.14	0.15	0.10	1392
Zr-REE-Silicate	0.23	0.27	0.19	0.24	0.27	2369
Fe-REE-Oxide	0.31	0.25	0.32	0.32	0.32	2978
Monazite	0.0039	0.0036	0.0011	0.0138	0.0002	45
Y-Arsenate	0.0000	0.0000	0.0042	0.0002	0.0013	11
REE-Y-Nb-Oxide	0.0006	0.0034	0.0011	0.0000	0.0017	15
Ca-Ti-Nb-REE-Oxide	0.20	0.23	0.24	0.17	0.17	2122
Ce-Allanite	0.02	0.05	0.01	0.02	0.02	279
CaTh-Silicate	0.00	0.02	0.01	0.01	0.01	110
Total	1.06	1.14	1.06	1.07	1.05	10,841

**Figure 4.** Ce and La distributions in REE-bearing minerals at different fractions.

In the SEM-BSE image of an albite particle locked with Fe-REE-Oxide (Figure 5), the liberation size of the Fe-REE-Oxide particle was around $-20 \mu\text{m}$. According to the EDS spectrum, Ce, La, Fe, Ti, Nb, Ca, Si, and O peaks were visible. Apart from the rare earth minerals, the Ag peak in EDS drew attention. The SEM-BSE image of a locked illite particle containing Zr-REE-Silicate is shown in Figure 6. The needle-like structure of the Zr-REE-Silicate mineral was also common in other SEM-BSE images. The liberation size of Zr-REE-Silicate particles was around $-20 \mu\text{m}$, and the EDS spectrum showed that Zr-REE-Silicate contained Ce, La, Zr, Nd, Fe, and Ca.

As shown in Figure 7, parisite was liberated around $-10 \mu\text{m}$ fraction and extremely locked by K-feldspar and quartz. Similarly to Zr-REE-Silicate, a needle-like structure was visible for parisite. The EDS spectrum indicated that it was one of the Y resources in the mineral composition in addition to Ce and La. According to Figure 8a, the bastnaesite was locked and entrapped by K-feldspar. Based on the image scale, bastnaesite seemed to be liberated under $20 \mu\text{m}$. The liberation size of the parisite encountered in the image was almost half that of the bastnaesite. In Figure 8b, Sr, Nd, and F elemental peaks were observed along with La and Ce.

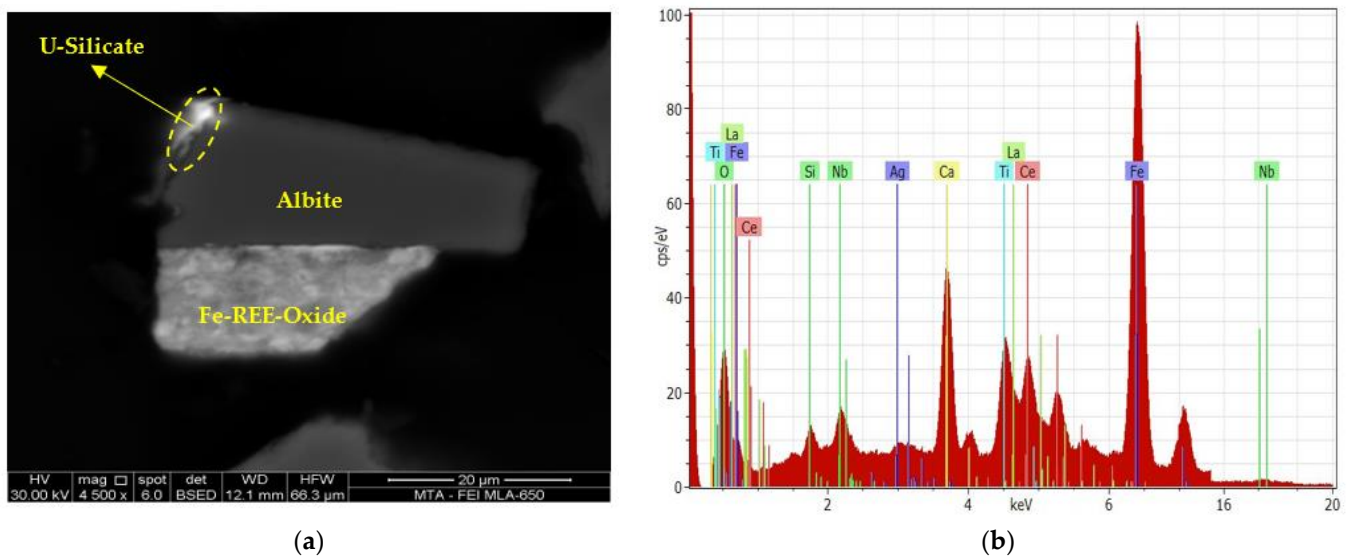


Figure 5. SEM-BSE image (a) and EDS spectrum (b) of Fe-REE-Oxide particle.

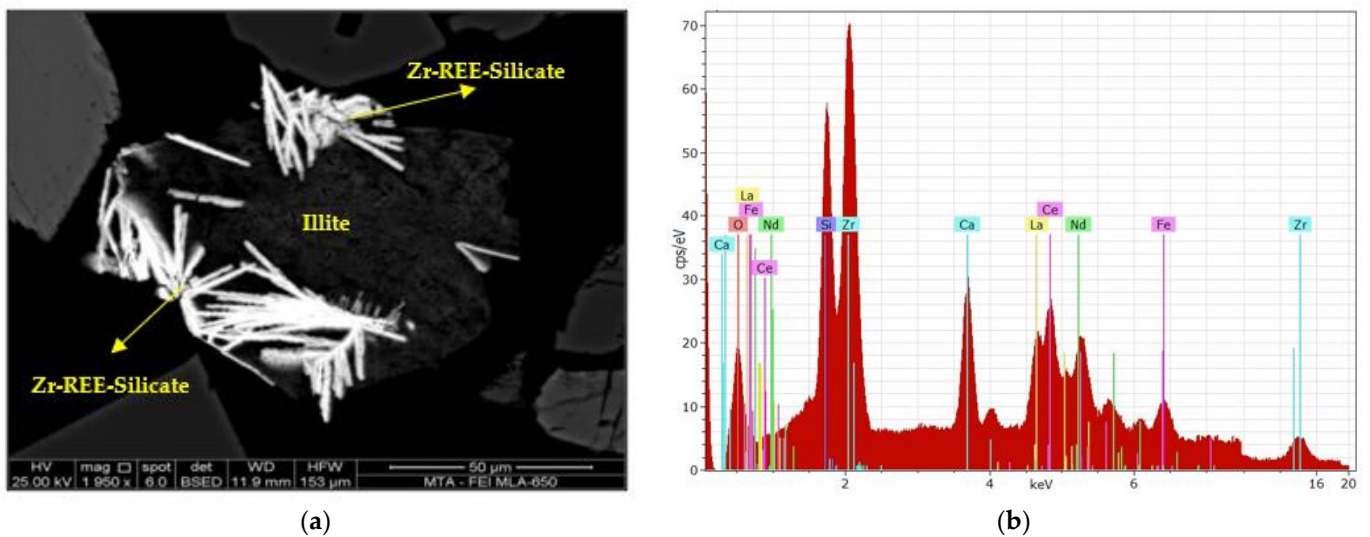


Figure 6. SEM-BSE image (a) and EDS spectrum (b) of Zr-REE-Silicate particle.

The liberation characteristics of individual particles and their associations between various minerals in the fractions were investigated. Due to the complex mineralogy of the deposit, REE-containing (Fe-REE-Oxide, Zr-REE-Silicate, parisite, and bastnaesite) particles were grouped for this analysis. The ratios of liberated, binary, and ternary particles for both fractions are summarized in Figure 9. Free particles of the main REE minerals are 11.63%, 12.25%, 9.82%, and 24.89%, respectively at the $-38 + 32 \mu\text{m}$ fraction, which indicates an insufficient liberation even in finer size fractions. Considering 11.63% is free for Fe-REE-Oxide particles, ~61% of Fe-REE-Oxide minerals are locked by gangue minerals in this size fraction, which the significant locking structure is associated with illite by 6.86% as binary and by 10.71% as ternary+, and also with biotite by 2.28% as binary and by 6.63% as ternary+.

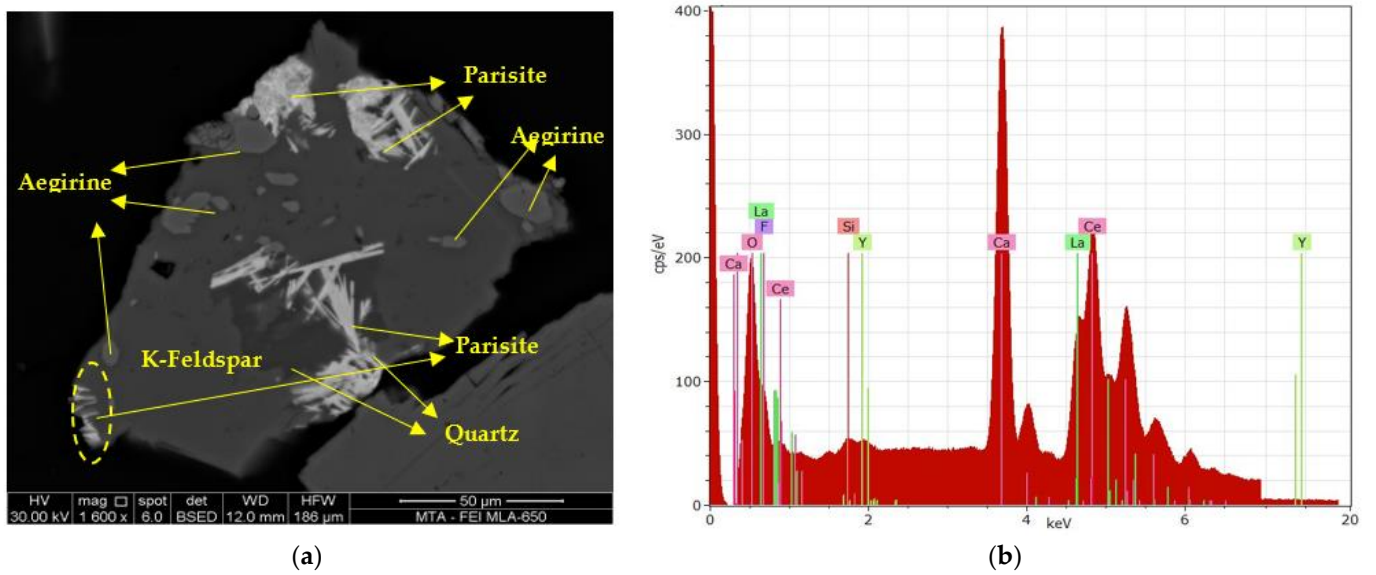


Figure 7. SEM-BSE image (a) and EDS spectrum (b) of parisite.

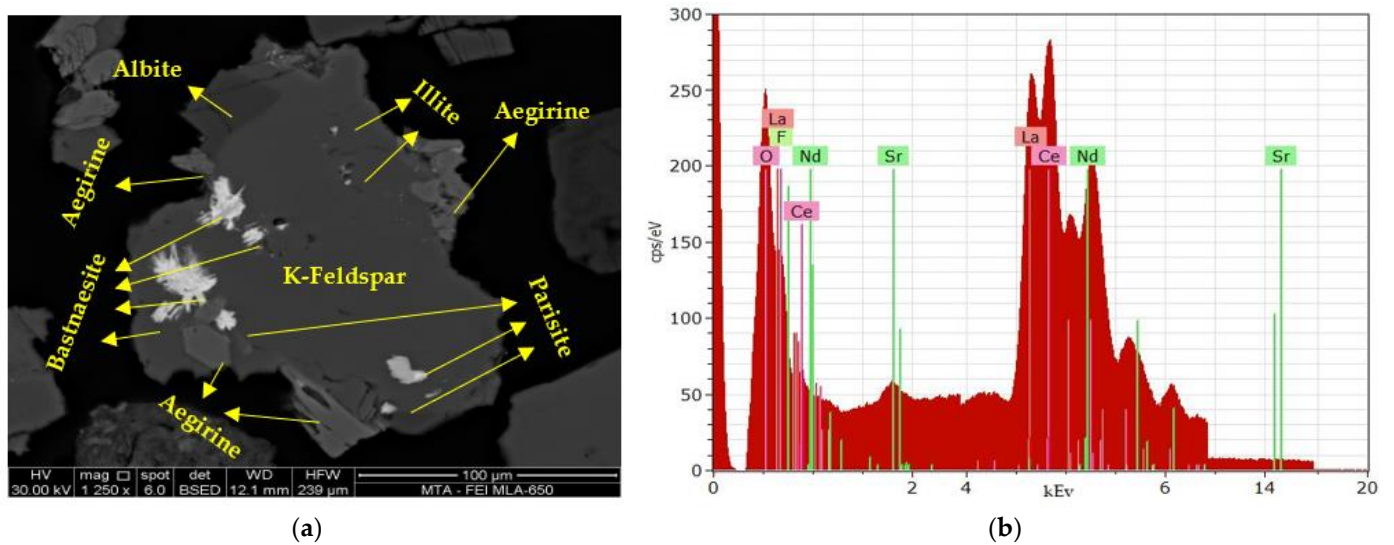


Figure 8. SEM-BSE image (a) and EDS spectrum (b) of bastnaesite.

According to Figure 9b, only 12.25% of Zr-REE-Silicates are free at the $-38 + 32 \mu\text{m}$ size fraction and $\sim 35\%$ of Zr-REE-Silicates are locked by other REE-bearing minerals, which means that $\sim 53\%$ of it is locked by gangue minerals as binary or ternary+ even in fine particle size. Zr-REE-Silicate particles are locked mainly with kaolinite by 4.28% as binary and by 1.08% as ternary+, with K-feldspar by 0.86% as binary and by 4.39% as ternary%, with calcite by 3.75% as binary and by 7.75% as ternary+ and also with illite by 2.16% as binary and by 11.01% as ternary+. It was concluded that illite had the highest locking ratio with Zr-REE-Silicate compared with other gangue minerals.

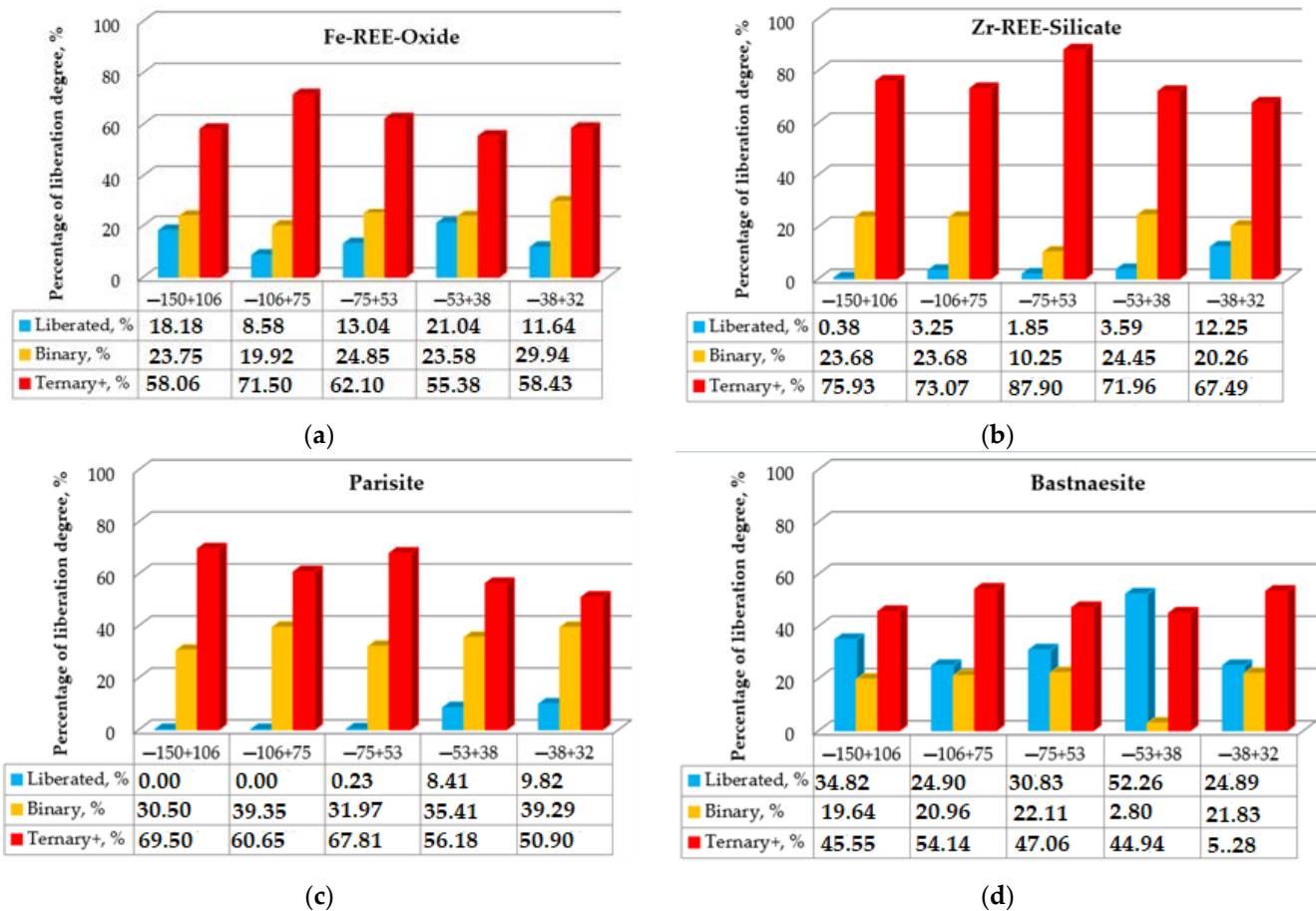


Figure 9. Liberation degree of Fe-REE-Oxide (a), Zr-REE-Silicate (b), parisite (c), and bastnaesite (d).

Roughly 65% of parisite particles are locked by gangue minerals in the $-38 + 32 \mu\text{m}$ fraction. K-feldspar, calcite, and illite have dominance on locking with parisite by 2.49% as binary and by 3.63% ternary+, by 15.01% as binary, and by 4.53% as ternary+ and by 6.14% as binary and by 10.65% as ternary+, respectively. Illite is one of the main gangue minerals interlocked with parisite. Bastnaesite particles have relatively higher liberation by 24.89%. Also, bastnaesite is locked by other REE-bearing minerals by $\sim 30\%$. As for gangue minerals, bastnaesite is mainly locked by K-feldspar, calcite, and fluorite by 3.92% as binary and by 5.40% as ternary+, by 7.64% as binary and by 2.15% as ternary+ and by 1.03% as binary and by 5.28%, respectively. Bastnaesite is locked by illite only by $\sim 5\%$ (binary + ternary+), which has a lower ratio compared to other REE-bearing minerals. In conclusion, REE-bearing minerals in the sample have a significant amount of locking ratio with Al-Fe silicates.

The free surface and minerals associations are illustrated in Figure 10. The free surface area of these four REE-bearing minerals increases towards fine fractions. Only bastnaesite decreased from about 40% to 35% after the $-53 + 38 \mu\text{m}$ fraction. If the results are evaluated in terms of free surface area, the order from the highest and the lowest will be bastnaesite > Fe-REE-Oxide > parisite > Zr-REE-Silicate. Fe-REE-Oxide is mostly locked with illite, while Zr-REE-Silicate is associated with illite and Ca-Zr silicates. While the parisite is mostly observed with Fe-REE-Oxide and Calcite, bastnaesite is bounded with Ca-Zr silicate, Zr-REE-silicate, and Fe-REE oxides. Fluoride is not detected in Fe-REE-Oxides. It is found locked with other REE-bearing minerals, especially with parisite and bastnaesite.

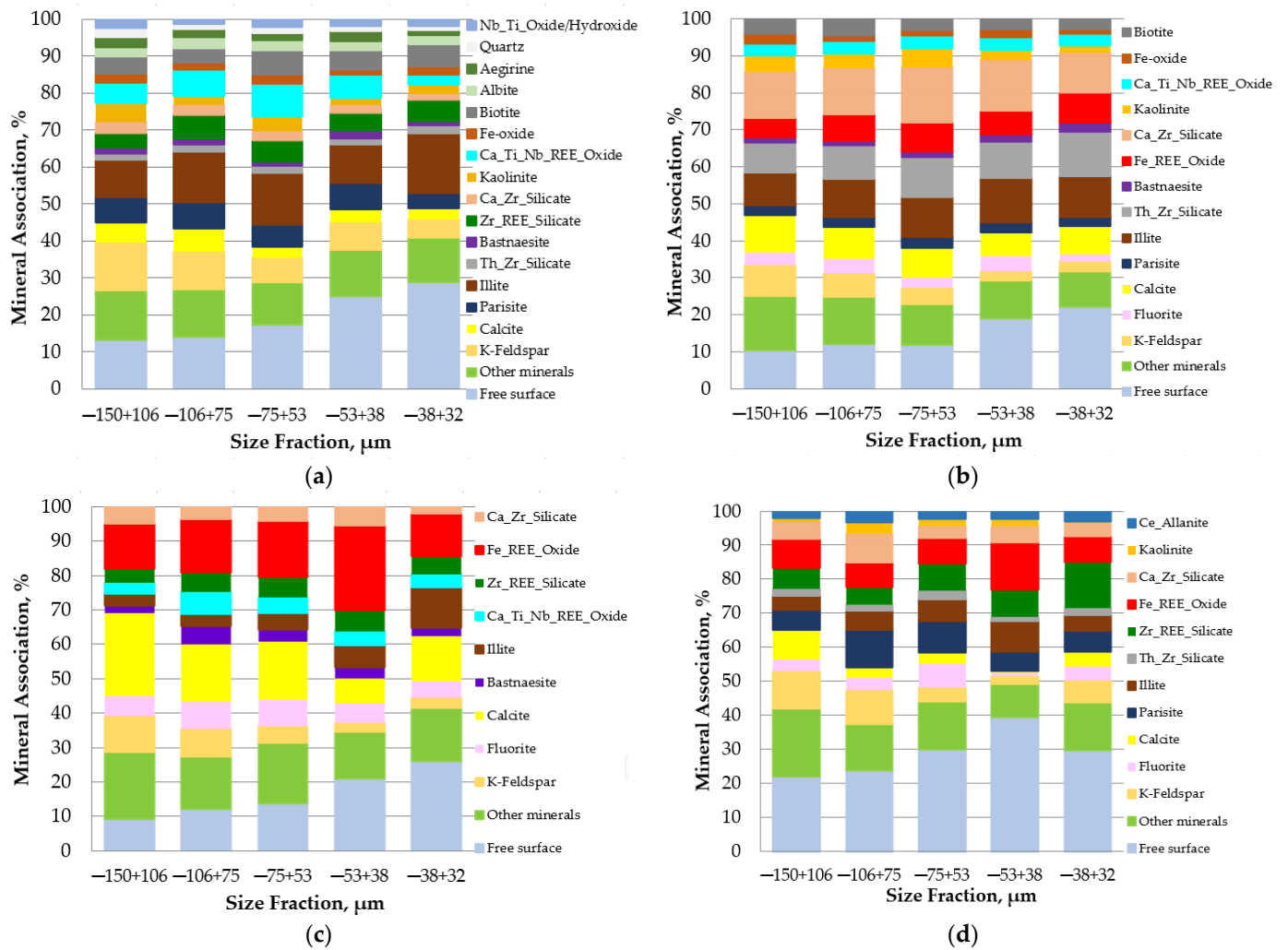


Figure 10. Mineral association and free surface ratios of Fe-REE-Oxide (a), Zr-REE-Silicate (b), parisite (c), and bastnaesite (d).

3.2. Beneficiation Studies

3.2.1. Shaking Table and MGS Experiments

To improve the efficiency of separation, the comminuted ore sample was classified into narrow size groups, and then shaking table separation was implemented on the $-1 + 0.3$ mm and $-0.3 + 0.074$ mm fractions. Using the -0.074 mm fraction, MGS experiments were performed in two stages by adjusting the rotational speed to 260 rpm and 200 rpm, respectively. The optimized parameters for MGS experiments were solids in a pulp ratio of 20%, washing water of 3.5 L/min, incline of 4° , feed rate of 2 L/min, and amplitude of 15 mm. The results of gravity separation at different fractions are given in Table 3.

As seen from Table 3, Σ REO contents of fractions decreased gradually from the coarsest to the finest. According to the result of the gravity separation for the coarsest fraction, about 11.3% by weight of the total feed was obtained as a heavy product containing 6437 g/t of Σ REO. Although the Σ REO content was lower compared to that of the coarsest fraction, a heavy product with higher Σ REO content was produced in the $-0.3 + 0.074$ mm fraction. These results confirm the MLA results. Mineral particles that contain REO become more liberated in fine fractions and concentrated in heavy products with higher Σ REO contents. Since the particle liberation of REE was below about 20 μm, Σ REO contents in light products could not be further reduced. In addition, the content of some major oxide minerals in ore composition showed important indications.

Table 3. The REO contents of gravity separation products.

Size Fraction, mm	Products	Amount, %	Content, g/t			Recovery, %
			LREO	HREO	∑REO	
−1 + 0.3	Heavy	11.3	5245	1192	6437	20.1
	Middling	13.6	3703	802	4505	16.8
	Light	26.7	2538	572	3110	22.8
	Total	51.6	3439	769	4207	59.7
−0.3 + 0.074	Heavy	2.1	6824	1499	8323	4.8
	Middling	7.0	2884	669	3553	6.8
	Light	12.9	1840	415	2255	9.0
	Total	22.0	2771	639	3410	20.6
−0.074	Heavy	14.5	2180	539	2719	10.8
	Middling	1.0	3176	846	4022	1.1
	Light	10.9	2014	587	2601	7.8
	Total	26.4	2149	570	2720	19.7
Total		100.0	2951	687	3639	100.0

As seen in Table 4 and Figure 11, the Na₂O content and recovery showed an increasing trend from light to heavy product. This situation was also very similar for U₃O₈ and ThO₂. In the heavy product of the coarse size, the ThO₂ and U₃O₈ contents increased to a limited extent; however, their increase at the finer fraction was more pronounced. The Fe₂O₃ content of the heavy product at the medium fraction increased almost three times compared to the feed. Although its specific gravity was higher than that of aluminum silicate minerals, due to its interlocking structure, minerals containing iron oxide were obtained from middling with a high Fe₂O₃ content (14.60%).

Table 4. Oxide contents of gravity separation experiments.

Size Fraction, mm	Products	Amount, %	Content, %									
			Na ₂ O	K ₂ O	SiO ₂	Al ₂ O ₃	Fe ₂ O ₃	TiO ₂	CaO	ZrO ₂	U ₃ O ₈	ThO ₂
−1 + 0.3	Heavy	11.3	7.88	2.77	57.02	15.51	1.84	0.27	5.97	0.85	0.042	0.052
	Middling	13.6	5.73	2.06	46.05	11.60	13.20	1.15	7.28	1.17	0.031	0.025
	Light	26.7	4.82	2.93	53.10	15.05	6.39	0.59	6.81	0.69	0.024	0.016
	Total	51.6	5.73	2.67	52.10	14.24	7.19	0.67	6.75	0.85	0.030	0.026
−0.3 + 0.074	Heavy	2.1	7.14	1.31	39.73	8.23	14.60	1.37	7.96	4.22	0.048	0.072
	Middling	7.0	8.07	2.52	54.09	13.22	5.11	0.74	7.53	0.84	0.024	0.021
	Light	12.9	7.14	3.02	56.01	15.33	3.74	0.44	6.43	0.52	0.021	0.015
	Total	22.0	7.43	2.70	53.84	13.98	5.21	0.62	6.93	0.98	0.024	0.022
−0.074	Heavy	14.5	9.23	1.66	52.71	11.52	11.20	0.82	5.82	0.95	0.020	0.016
	Middling	1.0	7.68	2.02	49.73	11.34	13.10	1.16	7.44	0.51	0.032	0.023
	Light	10.9	1.70	1.11	55.76	16.64	8.93	0.70	5.62	0.25	0.028	0.019
	Total	26.4	6.06	1.45	53.86	13.63	10.33	0.78	5.80	0.64	0.024	0.017
Total		100.0	6.19	2.35	52.95	14.02	7.58	0.69	6.54	0.82	0.027	0.023

Similarly, ∑REO content showed the same trend in the heavy product of the medium fraction. Considering that Fe-REE-oxide was one of the important REE-bearing minerals in the ore composition, this may be a valuable indication for observing the enrichment behavior of REEs. This situation was also quite similar for MnO. The ZrO₂ content, which did not increase in the heavy product at the coarse fraction, increased approximately four times the feed in the heavy product of the −0.3 + 0.074 mm fraction, similarly to that of Fe₂O₃. Considering that Zr-REE-silicate was another important REE-bearing mineral in the ore composition, both Fe-REE-oxide and Zr-REE-silicate showed a tendency to be concentrated in the heavy product of the medium fraction, although the weight ratio of

this product contributed less to the recovery. ZrO_2 -bearing mineral particles were liberated from others in finer sizes, and their concentration in the heavy product increased due to the high specific gravity difference. The reason for the high REO content in this fraction may have been due to the increased concentration of the Zr-REE-Silicate. In addition to these findings, the heavy product of the medium fraction gave the lowest SiO_2 content, which indicated lower concentrations of silicate gangues, while that of REE-bearing oxides was high.

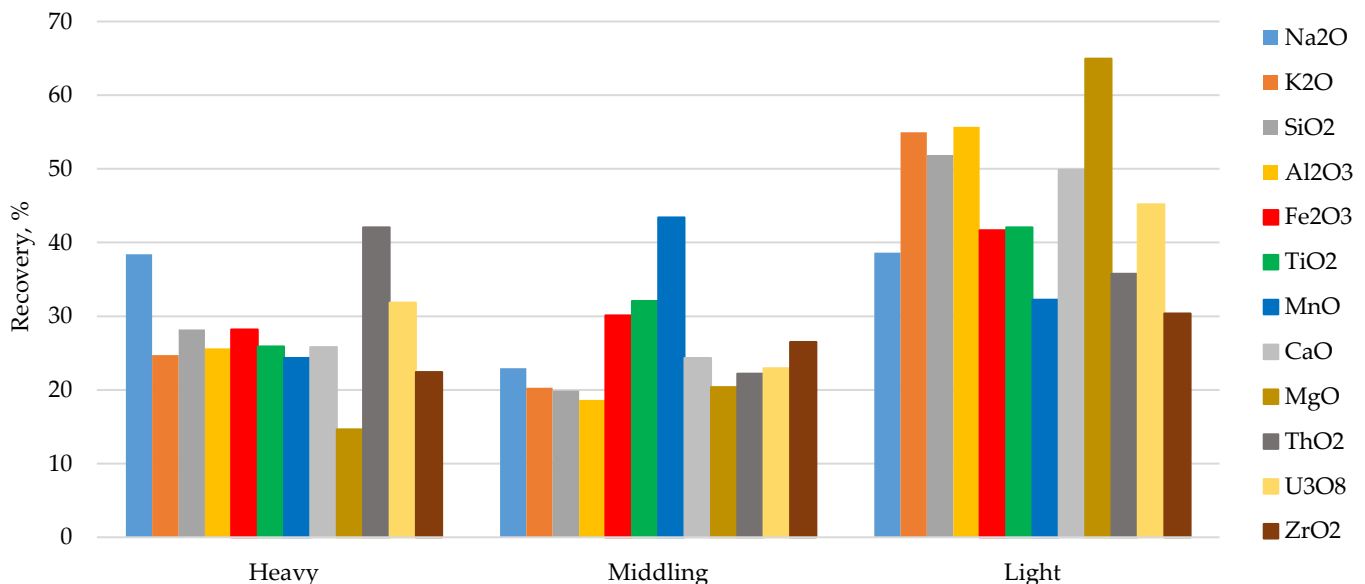


Figure 11. Total recoveries of major oxides after gravity separation.

Although Fe-REE-Oxide was one of the main REE-bearing minerals in the ore composition and its specific gravity was comparatively high, the Fe_2O_3 recovery rate was not the greatest in the heavy fraction. After gravity separation, a final heavy product weighing about 28% of the feed was obtained, whereas Na_2O and ThO_2 were distributed in the heavy product at a rate of 40% compared to other oxides. As seen in the SEM-BSE image in Figure 6a, the REE-bearing mineral Fe-REE-Oxide and Uranium silicate associated with the albite particle could explain the high Na_2O and REO content in the heavy product. In the light product, the high contents of MgO , K_2O , and Al_2O_3 were remarkable. This indicated the discharging of fined-sized clay and mica particles with a layered structure to the light product by the drag force of the flowing water film on the shaking table.

3.2.2. Centrifugal Separation Experiments

To increase the REE liberation degree and produce more liberated minerals, the run-of-mine ore was ground below $74\ \mu m$ and then subjected to centrifugal separators (MGS and Knelson) that employed high G-force to particles to be separated according to the specific gravity difference. MGS experiments were carried out under the optimum conditions of the previous tests. To obtain a product with higher REE contents, a Knelson concentrator that can reach higher rotational speeds was used. The solids-in-pulp ratio and the gravity force were adjusted to 10% and 80 G, respectively. Fluidization water was adjusted between 0.5 and 3 psi to produce a final heavy product. The results of centrifugal separation experiments are presented in Table 5.

Table 5. The REO contents of centrifugal separation tests.

Concentrator Type	Products	Weight, %	Content, g/t			Recovery, %
			LREO	HREO	Σ REO	
MGS	Heavy	57.0	3208	696	3904	61.7
	Middling	4.2	3328	817	4145	4.8
	Light	38.8	2448	666	3114	33.5
	Total	100.0	2919	690	3609	100.0
Knelson	Heavy	0.9	5349	1075	6424	1.5
	Middling	35.1	2742	689	3431	33.0
	Light	64.0	2972	767	3739	65.5
	Total	100.0	2912	742	3654	100.0

It can be noticed from Table 5 that the total REO content increased from the initial grade of 3609 g/t to 3904 g/t and 4145 g/t for the heavy and middling products, respectively. It is clear from the MGS test results that a much higher G-force might be required to capture REE-bearing minerals that are mixed into the middling and light products. To produce a heavy fraction with higher Σ REO content and recovery, the Knelson concentrator was introduced. In the first step, the fluidization water was adjusted to 0.5 psi to obtain a light product with low REO content. In the next step, the bulk heavy product was fed to the concentrator, and the fluidization pressure was increased to 3 psi. The increased fluidization water provided high fluid resistance that kept the particles from settling, and the amount of overflow product increased. By increasing the pressure to 3 psi, the particles that were not affected by 0.5 psi left the cone and were obtained as middlings. Σ REO grades of the heavy product increased to 6424 g/t. It was not possible to produce a heavy product with a high REE content using MGS and Knelson, since REE-bearing minerals, which are known to be liberated between 20 and 30 μ m, cannot be separated from host minerals and move together. The Knelson concentrator, which can generate much higher G forces than MGS, was able to concentrate a limited number of liberated REE-bearing particles in the heavy product. The recovery was also found to be quite low since a heavy product was obtained with an amount of 0.9% relative to the feed. These results showed that a selective separation was not even possible below 75 μ m.

The oxide contents of MGS products are given in Table 6. Since the amount of heavy product in the Knelson experiment was insufficient, the oxide contents could not be determined. The middlings had a relatively higher REO content than other products. If the contents of oxides in the same product were examined, it was seen that Fe₂O₃, TiO₂, CaO, and U₃O₈ showed the same trend. This tendency drew attention to the Ca-Ti-Nb-REE-Oxide and Ca-Th-Silicate mineral, which is found especially together with Fe-REE-Oxide, Zr-REE-Silicate, and parasite minerals (see Figure 11).

Table 6. Oxide contents of MGS products.

Products	Amount, %	Content, %								
		Na ₂ O	K ₂ O	SiO ₂	Al ₂ O ₃	Fe ₂ O ₃	TiO ₂	CaO	U ₃ O ₈	ThO ₂
Heavy	11.3	8.09	2.79	52.51	12.06	7.59	0.68	6.60	0.026	0.027
Middling	13.6	7.77	2.59	50.98	11.65	8.86	0.90	7.88	0.031	0.024
Light	26.7	2.85	1.69	54.29	17.04	7.51	0.65	6.09	0.029	0.021
Total	100.0	6.05	2.36	53.17	13.98	7.62	0.68	6.46	0.027	0.024

The distributions of oxides in the MGS products are shown in Figure 12. Sodium and potassium alumina silicates and iron silicates were mainly distributed in the heavy product. Similarly to the results of the previous gravity experiments, the light product contained high levels of MgO and Al₂O₃, but the level of K₂O was quite low. These results may indicate that clinocllore, another mica mineral that is fragmented by alteration and

distributed in finer sizes, was present in the light product rather than muscovite grains. Illite was another major gangue mineral locking REE-bearing minerals, according to the MLA results. Considering higher Σ REO, Fe_2O_3 , and K_2O contents in the middling product, the structures consisting of an illite matrix in particles (see Figure 6) could be the reason for this REE concentration. Also, parisite, REE fluoro carbonate containing Ca, could be another mineral that was concentrated in the middling product.

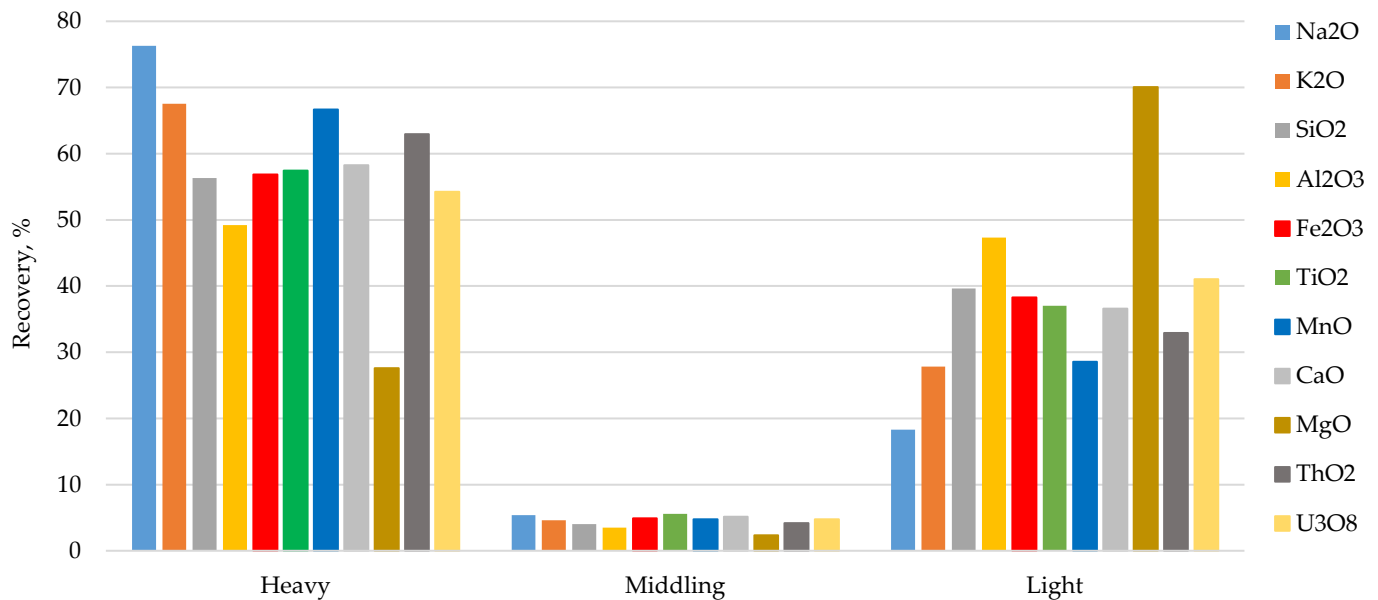


Figure 12. Total recoveries of major oxides after MGS.

3.2.3. Magnetic Separation Experiments

Magnetic separation experiments were conducted on the $-1 + 0.3$ mm and the $-0.3 + 0.074$ mm fractions. The band speed of REMS was set as 100 rpm, and the angles of splitters were adjusted to 95° – 110° for coarse fractions. For the fine fraction, the band speed was increased to 110 rpm, and the angles of the splitters were adjusted to 90° – 110° . The results of the magnetic separation tests are given in Table 7.

Table 7. The REO contents based on magnetic separation tests.

Size Fraction, mm	Products	Weight, %	Content, g/t			Recovery, %
			LREO	HREO	Σ REO	
$-1 + 0.3$	Magnetic	20.6	4464	1097	5561	31.6
	Middling	11.3	3662	838	4500	13.9
	Non-Magnetic	19.7	2109	489	2598	14.1
	Total	51.6	3389	808	4198	59.6
$-0.3 + 0.074$	Magnetic	6.7	5005	1008	6013	11.1
	Middling	4.7	2600	595	3195	4.2
	Non-Magnetic	10.5	1449	375	1823	5.3
	Total	22.0	2786	616	3402	20.6
-0.074		26.4	2149	570	2720	19.8
Total		100.0	2929	703	3633	100.0

As seen in Table 7, although the $-1 + 0.3$ mm fraction contained more REO, a magnetic product with a lower REO content was obtained due to insufficient liberation. About 20.6% by weight of the total feed was obtained as a magnetic product containing 5561 g/t of Σ REO. With the increased liberation of REE-bearing minerals with magnetic properties, the content of nonmagnetic product decreased to around 1800 g/t. The reason for this low recovery

was that some REE-bearing minerals were associated with non-magnetic (e.g., calcite, silicates) minerals. Similar results for the Fe recovery were recorded from the Ashram deposits; 69.7% of Fe-bearing minerals were concentrated in the magnetic fraction using a wet high-intensity magnetic separator (WHIMS) at 4000 Gauss [23]. The reason for this low recovery is explained by the presence of some bastnaesite and monazite grains bounded with non-magnetic (e.g., dolomite, fluorite) minerals, thus reducing their magnetic fraction pre-concentration potential. As seen in Table 8, there was not much difference in the ZrO₂ content in the coarse fraction; however, it increased to 1.47% in the nonmagnetic product of the finer fraction. Due to the presence of REE-bearing minerals such as Zr-REE-Silicate with nonmagnetic properties, magnetic separation tests remained limited.

Table 8. Oxide contents based on magnetic separation test.

Size Fraction, mm	Products	Amount, %	Content, %									
			Na ₂ O	K ₂ O	SiO ₂	Al ₂ O ₃	Fe ₂ O ₃	TiO ₂	CaO	ZrO ₂	U ₃ O ₈	ThO ₂
−1 + 0.3	Magnetic	20.6	6.86	2.09	49.08	11.66	12.41	0.83	4.97	0.82	0.024	0.031
	Middling	11.3	5.65	3.47	54.50	15.77	2.39	0.40	7.67	0.86	0.035	0.031
	Non-Magnetic	19.7	4.51	3.04	53.04	15.66	4.49	0.67	7.35	0.94	0.033	0.018
	Total	51.6	5.70	2.75	51.77	14.08	7.20	0.68	6.47	0.87	0.030	0.026
−0.3 + 0.074	Magnetic	6.7	4.42	2.28	55.13	15.95	7.18	0.84	8.41	0.61	0.028	0.036
	Middling	4.7	9.73	2.45	60.71	17.54	1.43	0.21	5.37	0.42	0.024	0.020
	Non-Magnetic	10.5	8.23	2.58	50.07	10.84	6.30	0.64	6.78	1.47	0.021	0.014
	Total	22.0	7.38	2.46	53.91	13.85	5.52	0.61	6.98	0.98	0.024	0.022
−0.074		26.4	6.12	1.56	53.72	13.72	10.52	0.76	5.85	0.65	0.026	0.018
Total		100.0	6.18	2.37	52.76	13.94	7.71	0.68	6.42	0.84	0.027	0.023

The distributions of oxides in the magnetic separation products are presented in Figure 13. After magnetic separation, a final magnetic product weighing about 27.5% of the feed was concentrated. Fe₂O₃, MnO, TiO₂, and MgO had significant recovery peaks in the magnetic product at rates of 39.5%, 43.2%, 33.4%, and 33.5%, respectively. In particular, the increase in Fe and Mg contents in the magnetic product at the fine fraction could be due to the transportation of the layered iron-bearing muscovite particles that adhered to the band of the separator. Furthermore, high CaO and TiO₂ contents, especially in the magnetic product of the fine fraction, might be an indication of Titanite and Ca-Ti-Nb-REE-oxide. Also, both ZrO₂ content and recovery reached maximums in the non-magnetic product, and the increase in content and significant recovery peak could be indications for Zr-REE-silicate. Based on these results, it is difficult to separate REE-bearing minerals associated with non-magnetic or paramagnetic minerals from the non-magnetic fraction.

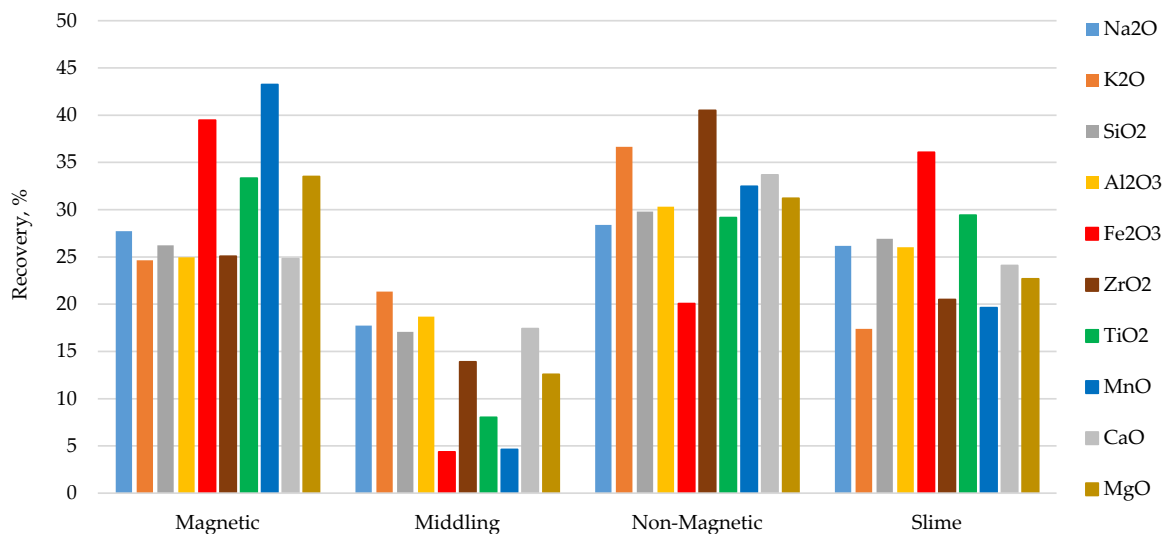


Figure 13. Total recoveries of major oxides after magnetic separation.

4. Conclusions

In this study, the detailed characterization of Malatya/Kuluncak REE ore was completed by performing PSD, chemical, MLA, XRD, and SEM-EDS analyses. Physical beneficiation equipment such as a shaking table, centrifugal (MGS and Knelson) and magnetic separation were used for the beneficiation of REEs. Based on the characterization and descriptive enrichment studies, the obtained results are summarized as follows:

Malatya/Kuluncak ore contained 2932 g/t LREO and 696 g/t HREO, which means light REEs were more dominant. Approximately 237 g/t ThO₂ and 272 g/t U₃O₈ were detected as radioactive elements. The XRD studies indicated that the ore was mostly composed of albite, calcite, montmorillonite, muscovite, titanite, kaolinite, clinocllore, and aegirine. The modal mineralogical composition was defined through MLA, and the dominant gangue minerals in the ore composition were alumina-silicates and iron-silicates such as albite, K-feldspar, and aegirine.

The novel part of the characterization studies was that from the EDS results, Fe-REE-Oxide, Zr-REE-Silicate, Bastnaesite, Parisite, and Ca-Ti-Nb-REE-Oxide were identified as the main REE-bearing minerals. According to the SEM-BSE analysis, while Fe-REE-Oxides were locked with albite, Zr-REE-Silicates were associated with illite. Parisite and Bastnaesite were mostly observed together with K-feldspar. MLA detected that free REE-bearing mineral particles were present in low percentages even in the size fraction of $-38 + 32 \mu\text{m}$. SEM-BSE images contributed to this finding and showed that the liberation size of the abovementioned REE-bearing minerals was around $-20 \mu\text{m}$. The complex structure is thought to be liberated by grinding down to about $30 \mu\text{m}$, which means enrichment tests should be carried out at fine-ultrafine particle sizes.

After shaking table separation, a final heavy product weighing about 28% of the feed was obtained, whereas Na₂O and ThO₂ were distributed in the heavy product at a rate of 40% compared to other oxides. Fe-REE-Oxide and Uranium silicate associated with the albite particle could explain the high Na₂O and REO content in the heavy product. In the light product, the high content of MgO, K₂O, SiO₂, and Al₂O₃ indicated the fine-sized clay and mica particles with a layered structure were mainly discharged to the light product. After centrifugal separation tests, the Σ REO grade of the heavy product increased to 6424 g/t; however, the light product of the Knelson concentrator in particular contained a high amount of REO. These results showed that selective separation was not even possible below $75 \mu\text{m}$ size.

About 20.6% by weight of the total feed was obtained as a magnetic product with a Σ REO content of 5561 g/t. With the increased liberation of REE-bearing minerals with magnetic properties, the content of nonmagnetic product decreased to around 1800 g/t, and a magnetic product containing 6013 g/t Σ REO was obtained. Fe₂O₃, MnO, TiO₂, and MnO showed significant recovery peaks in the magnetic product. This trend is important since Fe and Ti oxides are associated with REE-bearing minerals in the ore composition. Zr had the highest peak in the non-magnetic product; thus, magnetic separation remained limited for REO enrichment.

In conclusion, the physical enrichment results for Malatya/Kuluncak REE ore showed that the production of a pre-concentrate with high REO content would be very limited. The biggest challenge here was that there was more than one REE-bearing mineral structure having different physical and chemical properties with a very low liberation size. However, mineralogy parameters obtained by MLA provided good guidance for further improvement of the enrichment process. It is recommended that future studies should be carried out with physicochemical enrichment or direct chemical treatments using very fine fractions.

Author Contributions: B.E., M.U.B. and F.B. contributed to the investigation, methodology, and experimental design. B.E. and F.B. wrote the paper. F.B., S.T. and B.S.S. were involved in supervision, validation, visualization, review, and editing. All authors have read and agreed to the published version of the manuscript.

Funding: The present study is based on the results of the MSc thesis conducted at the Istanbul Technical University and was funded by the BAP (Scientific Research Project) Department with grant number 42931.

Data Availability Statement: Not applicable.

Acknowledgments: The authors sincerely thank the Mineral Processing Engineering Department for providing laboratory equipment. We would like to thank TENMAK/NATEN for supplying the sample and financial support for MLA and chemical analysis, the General Directorate of Mineral Research and Exploration (MTA) and Okan PULAT, senior geologist of the exploration team of the project area, for their support in the site visit and basic information about the geology of the project area, and Nihal Görmüş for her contribution to the MLA analysis and data interpretation.

Conflicts of Interest: The authors declare no conflict of interest.

References

1. Krishnamurthy, N.; Gupta, C.K. *Extractive Metallurgy of Rare Earths*, 2nd ed.; CRC Press: Boca Raton, FL, USA, 2005. [CrossRef]
2. Yang, X.; Satur, J.V.; Sanematsu, K.; Laukkanen, J.; Saastamoinen, T. Beneficiation studies of a complex REE ore. *Miner. Eng.* **2015**, *71*, 55–64. [CrossRef]
3. Barteková, E.; Kemp, R. National strategies for securing a stable supply of rare earths in different world regions. *Resour. Policy* **2016**, *49*, 153–164. [CrossRef]
4. USGS. Rare Earths, Mineral Commodity Summaries. 2023. Available online: <https://pubs.usgs.gov/periodicals/mcs2023/mcs2023.pdf> (accessed on 25 May 2023).
5. Weng, Z.; Jowitt, S.M.; Mudd, G.M.; Haque, N. A Detailed Assessment of Global Rare Earth Element Resources: Opportunities and Challenges. *Econ. Geol.* **2015**, *110*, 1925–1952. [CrossRef]
6. Polat, E.G.; Yücesan, M.; Gül, M. A comparative framework for criticality assessment of strategic raw materials in Turkey. *Resour. Policy* **2023**, *82*, 103511. [CrossRef]
7. Özgenc, İ.; Kibici, Y. Başören köyü (Kuluncak-Malatya) Britolit damarlarının jeolojisi ve kimyasal-mineralojik özellikleri. *Türkiye Jeol. Bülteni* **1994**, *7*, 77–85.
8. Akıska, E.; Karakaş, Z.; Öztürk, C. Uranium, Thorium and Rare Earth Element Deposits of Turkey. In *Mineral Resources of Turkey*; Pirajno, F., Ünlü, T., Dönmez, C., Şahin, M., Eds.; Modern Approaches in Solid Earth Sciences; Springer: Cham, Switzerland, 2019; p. 19. [CrossRef]
9. Pulat, O.; Karakaş, M.; Yastı, M.A. Relationship of ore properties and alteration of the Büyük Kuluncak (Malatya) Nb- U-NTE-Zr-Li deposit. *Bull. Miner. Res. Explor.* **2022**, *167*, 127–148.
10. Jordens, A.; Cheng, Y.P.; Waters, K.E. A review of the beneficiation of rare earth element bearing minerals. *Miner. Eng.* **2013**, *41*, 97–114. [CrossRef]
11. Burat, F.; Baştürkcü, H.; Özer, M. Gold & silver recovery from jewelry waste with combination of physical and physicochemical methods. *Waste Manag.* **2019**, *89*, 10–20. [CrossRef]
12. Mennik, F.; Dinç, N.İ.; Burat, F. Selective recovery of metals from spent mobile phone lithium-ion batteries through froth flotation followed by magnetic separation procedure. *Results Eng.* **2023**, *17*, 100868. [CrossRef]
13. Celep, O.; Yazıcı, E.Y.; Deveci, H. Production of rare earth elements from primary and secondary resources. *GÜFBED/GUSTIJ* **2021**, *11*, 264–280.
14. Chi, R.; Xu, S.; Zhu, G.; Xu, J.; Qiu, X. Beneficiation of rare earth ore in china. In *Light Metals 2001: Technical Sessions at the 130th TMS Annual Meeting*; Anjier, J.L., Ed.; TMS Aluminum Committee: New Orleans, LA, USA, 2001; pp. 1159–1165.
15. Luo, J.; Chen, X. Research into the recovery of high-grade rare-earth concentrate from Baotou complex iron ore, China. In *Mineral Processing and Extractive Metallurgy*; Jones, M.J., Gill, P., Hui, Z.J.S.X., Eds.; IMM and Chinese Society of Metals: Kunming, China, 1984; pp. 663–675.
16. Ozbayoglu, G.; Atalay, U. Beneficiation of bastnaesite by a multi-gravity separator. *J. Alloys Compd.* **2000**, *303–304*, 520–523. [CrossRef]
17. Jordens, A.; Sheridan, R.S.; Rowson, N.A.; Waters, K.E. Processing a rare earth mineral deposit using gravity and magnetic separation. *Miner. Eng.* **2014**, *62*, 9–18. [CrossRef]
18. Dehaine, Q.; Filippov, L.O. Rare earth (La, Ce, Nd) and rare metals (Sn, Nb, W) as by-product of kaolin production, Cornwall: Part 1: Selection and characterisation of the valuable stream. *Miner. Eng.* **2014**, *76*, 141–153. [CrossRef]
19. Zhang, J.; Zhao, B.; Schreiner, B. *Separation Hydrometallurgy of Rare Earth Elements*; Springer: Cham, Switzerland, 2016. [CrossRef]
20. Gupta, C.K.; Krishnamurthy, N. Extractive metallurgy of rare earths. *Int. Mater. Rev.* **1992**, *37*, 197–248. [CrossRef]
21. Habashi, F. Extractive metallurgy of rare earths. *Can. Metall. Q.* **2013**, *52*, 224–233. [CrossRef]
22. Jordens, A.; Marion, C.; Langlois, R.; Grammatikopoulos, T.; Rowson, N.A.; Waters, K.E. Beneficiation of the Nechalacho Rare Earth Deposit. Part 1: Gravity and Magnetic Separation. *Miner. Eng.* **2016**, *99*, 111–122. [CrossRef]
23. Nguyen, T.Y.C.; Tran, L.H.; Mueller, K.K.; Coudert, L.; Mercier, G.; Blais, J.F. Pre-concentration of fluorite from a rare earth element carbonatite deposit through the combination of magnetic separation and leaching. *Miner. Eng.* **2021**, *174*, 106998. [CrossRef]

24. Thompson, W.; Lombard, A.; Santiago, E.; Sing, A. Mineralogical Studies in Assisting Beneficiation of Rare Earth Element Minerals from Carbonatite Deposits. In Proceedings of the 10th International Congress for Applied Mineralogy (ICAM), Trondheim, Norway, 1–5 August 2011; Springer: Berlin/Heidelberg, Germany, 2012; pp. 665–672.
25. Hedrick, J.B.; Sinha, S.P.; Kosynkin, V.D. Loparite, a rare-earth ore (Ce, Na, Sr, Ca)(Ti, Nb, Ta, Fe+3)O₃. *J. Alloys Compd.* **1997**, *250*, 467–470. [[CrossRef](#)]
26. Fuerstenau, D.W.; Pradip. Zeta potentials in the flotation of oxide and silicate minerals. *Adv. Colloid Interface Sci.* **2005**, *114–115*, 9–26. [[CrossRef](#)]
27. Ulusoy, U.A. Review of particle shape effects on material properties for various engineering applications: From macro to nanoscale. *Minerals* **2023**, *13*, 91. [[CrossRef](#)]
28. Xu, C.; Zhong, C.; Lyu, R.; Ruan, Y.; Zhang, Z.; Chi, R. Process mineralogy of Weishan rare earth ore by MLA. *J. Rare Earths* **2019**, *37*, 334–338. [[CrossRef](#)]
29. Baştürkçü, E.; Şavran, C.; Yüce, A.E.; Timur, S.İ. Revealing the effects of mechanical attrition applied on Eskisehir-Beylikova REE ore utilizing MLA. *Miner. Eng.* **2022**, *186*, 107733. [[CrossRef](#)]

Disclaimer/Publisher’s Note: The statements, opinions and data contained in all publications are solely those of the individual author(s) and contributor(s) and not of MDPI and/or the editor(s). MDPI and/or the editor(s) disclaim responsibility for any injury to people or property resulting from any ideas, methods, instructions or products referred to in the content.